Universität Rostock
Traditio et Innovatio

ATTAVANTI: Multiphysical Shape Optimization of a QPR under Uncertainties

focus on E-S-T coupled problem under uncertainty

Piotr Putek[1], Simon B. Adrian[1], Ursula van Rienen[1,2], Marc Wenskat[4] and Shahnam Gorgi Zadeh[4]

University of Rostock,
[1]Institute of General Electrical Engineering,
[2]Department of Life, Light & Matter
[3]University of Hamburg & DESY
[4]CERN, Geneva,

Outline

Outline

Outline

Outline

Outline

Timeline of ATTAVANTI subproject

Multiphysical Shape Optimization of a QPR under Uncertainties

AP	Aufgabe	2021		2022				2023				2024	
		3	4	1	2	3	4	1	2	3	4	1	2
3.1	Modeling of the electromagnetic-stress-heat coupled problem of the QPR under uncertainties												
3.2	Analysis of the existing QPR design to understand the detuning mechanism and microphonics												
3.3	Stochastic MO (parametric) design optimization of the QPR under coupling												
3.4	Topology optimization of the pole shoes for a homogeneous penetration of the sample												

Nr.	Zieldatum (Quartal/Jahr)	Beschreibung der Meilensteine von AP 3
1	I / 2022	Modeling of the electromagnetic-stress-heat coupled problem of the QPR under uncertainties
2	IV / 2022	Analysis of the existing QPR design to understand the detuning mechanism and microphonics
3	III / 2023	Stochastic MO (parametric) design optimization of the QPR under coupling
4	II / 2024	Topology optimization of the pole shoes for homogeneous penetration of the sample

1st interim report: IV. 22

2nd interim report: IV. 23

Electro-Stress-Thermal (E-S-T) Shape Optimization

A fast model with sufficiently good accuracy

- CST Studio Suite®: unidirectional stochastic coupled (E-S-T) problem in steady state
- Static Lorentz force: scaled by a factor to mimic dynamic Lorenz force based on simulation in time domain in COMSOL®
- Trade-off between computational time & accuracy due to the Pareto-front framework
- Due to the multi-objective steepest descent method: shape derivative of mean & variance for all the merit functions incl. max. temperature

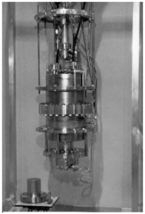

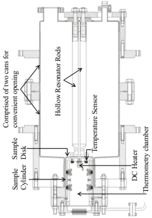

Illustration of the CERN-QPR [MCCHT03, J12]

Reliable & predictable simulations of QPRs

Uncertainty Quantification (UQ) studies of QPR:

- Material and geometric imperfections
- QPR model in steady state incl. broken symmetry of rods
- Local and global sensitivity without any additional effort

Exact methods to compute shape derivative not implemented in CST Studio®:

- Slater formula for only shift of frequency
- Lack of discrete/continuum design sensitivity analysis (DSA)
- Lack of inhomogeneous boundary conditions in Maxwell's eigenvalue problem formulation or access to mass and stiffness matrices

UQ-based worst-case analysis for multi-physics simulations of QPRs

Algorithmic complexity for shape derivatives of N objectives:

- Discrete/continuous DSA: $2 \cdot (N + 1) \cdot Q$ compared to developed method: $2 \cdot Q$ with Q denoted parameters number

Timeline of ATTAVANTI subproject

Problems & motivation

Stochastic modeling of coupled problem
- Parametrized QPR model
- Unidirectional Stochastic Coupled Problem

UQ-based worst-case analysis for multi-physics QPR simulations
- Influence of shape variations by Taylor expansion
- UQ-based worst-case method

Preliminary results & Conclusions
- Proof-of-concept example
- Results for PDFs of merit-function due to QPR deformation

Parametrized model of QPRs

A three-dimensional model (3D)

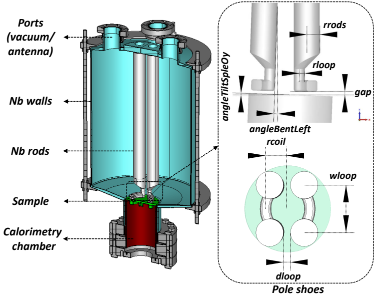

Layout of QPR [PZWHR19]

Name (mm)	CERN	HZB	SolA	SolA	stdDev
p_1(gap)	0.70	0.5	0.58	0.55	0.05
p_2(rrods)	15.00	13.0	9.76	9.14	0.05
p_3(hloop)	10.00	10.0	9.72	9.64	0.05
p_4(rloop)	8.00	5.0	5.92	5.56	0.05
p_5(wloop)	40.93	44.0	43.79	43.79	0.05
p_6(dloop)	5.00	6.0	4.0	4.0	0.05
p_7(rcoil)	23.00	22.40	25.00	25.00	0.05
p_8(rsample)	37.50	37.5	35.00	35.00	0.05
p_9(aBentRight)	0	0	0	0	0.25
p_{10}(aBentLeft)	0	0	0	0	0.25

$$R_S(\mathbf{p}) \doteq \frac{2\,[P_{\mathrm{DC1}}(\mathrm{p}) - P_{\mathrm{DC2}}(\mathrm{p})]}{\int_{\Omega_S} \|\mathrm{H}(\mathrm{p})\|^2 \, \mathrm{dx}} \tag{1}$$

where p : geometrical parameters, P_{DC1} & P_{DC2} : heater power at equilibrium for T_{int} and reduced heater power P_{DC2} after switching on RF antenna, **H** : magnetic field

Target values for functioning QPR

Basic functions of merit: $m = 1, \ldots, 3$; $k = 1, \ldots, 6$; $\mathbf{p} = (p_1, \ldots, p_Q)$

– Operating frequencies $[\mathrm{GHz}]$:

$$y_{1,1}(\mathbf{p}) = 0.429\ [\mathrm{GHz}], \quad y_{1,2}(\mathbf{p}) = 0.866\ [\mathrm{GHz}], \quad y_{1,3}(\mathbf{p}) = 1.3\ [\mathrm{GHz}],$$

– Focusing factor $[\mathrm{A}^2/\mathrm{J}]$:

$$y_{2,m}(\mathbf{H};\mathbf{p}) \doteq \frac{1}{2U} \int_{\Omega_\mathrm{S}} \|\mathbf{H}\|^2 \, \mathrm{d}x,$$

– Homogeneity factor $[1/1]$:

$$y_{3,m}(\mathbf{H};\mathbf{p}) \doteq \frac{\int_{\Omega_\mathrm{S}} \|\mathbf{H}\|^2 \, \mathrm{d}x}{|\Omega_\mathrm{S}| \max\limits_{\mathbf{x}\in\Omega_\mathrm{S}} (\|\mathbf{H}\|^2)},$$

– Operating range $[1/1]$:

$$y_{5,m}(\mathbf{H};\mathbf{p}) \doteq \frac{\max\limits_{\mathbf{x}\in\Omega_\mathrm{S}} (\|\mathbf{H}\|)}{\max\limits_{\mathbf{x}\in\Omega_\mathrm{R}} (\|\mathbf{H}\|)},$$

– Risk of field emission $[\mathrm{mT}/(\mathrm{MV}/\mathrm{m})]$:

$$y_{6,m}(\mathbf{H};\mathbf{p}) \doteq \frac{\mu_0 \max\limits_{\mathbf{x}\in\Omega_\mathrm{S}} (\|\mathbf{H}\|)}{\max\limits_{\mathbf{x}\in\Omega_\mathrm{R}} (\|\mathbf{E}\|)},$$

– Dimensionless factor (to study meas. bias) $[1/1]$:

$$y_{4,m}(\mathbf{H};\mathbf{p}) \doteq \frac{\int_{\Omega_\mathrm{S}} \|\mathbf{H}\|^2 \, \mathrm{d}x}{\int_{\Omega_\mathrm{F}} \|\mathbf{H}\|^2 \, \mathrm{d}x},$$

where **E**: electric field, Ω_S: surface of sample, Ω_R: domain of rods, Ω_F: domain of flange

Unidirectional Stochastic E-S-T coupled problem

A full three-dimensional model (3D):

$$\nabla \times \nabla \times \mathsf{E}(\theta) - \omega^2(\theta)\,\mu(\theta)\,\epsilon(\theta)\mathsf{E}(\theta) = 0, \qquad \text{in } D_\mathrm{c} \tag{2a}$$

$$\nabla \cdot \underbrace{\Big(\eta(\theta)(\nabla \mathsf{u}(\theta) + \nabla \mathsf{u}(\theta)^\top) + \lambda(\theta)\mathsf{I}\nabla \cdot \mathsf{u}(\theta)\Big)}_{=:\sigma(\theta)} = 0, \qquad \text{in } D_\mathrm{w} \tag{2b}$$

$$\nabla \cdot \kappa(\theta)\,\nabla T(\theta) + \gamma(\theta)|\mathsf{E}(\theta)|^2 = 0, \qquad \text{in } D_\mathrm{w} \tag{2c}$$

with radiation pressure $t(\theta)$ defined as: (2d)

$$\sigma(\theta) \cdot \mathsf{n}_\mathrm{w} = \underbrace{\frac{1}{4}\left(\epsilon|\mathsf{E}(\theta)|^2 + \frac{1}{\omega^2\mu}|\nabla \times \mathsf{E}(\theta)|^2\right)}_{=:t(\theta)} \cdot \mathsf{n}_\mathrm{w}, \qquad \text{on } \partial D_\mathrm{cw} \tag{2d}$$

for $\theta = (\mathsf{x}, f, \mathsf{p}) \in D \times \mathcal{F} \times \Pi$, $\quad \partial D = \partial D_\mathrm{D} \cup \partial D_\mathrm{N}$, $\quad \mathsf{p} = (p_1, \ldots, p_Q) \in \Pi \subset \mathbb{R}^Q$,
with $D \in \mathbb{R}^3$: computational domain, $\mathcal{F} \in \mathbb{R}$: frequency range, Π: parameter domain,
γ: electric conductivity, μ: magnetic permeability, ϵ: electric permittivity, ω: angular frequency
η, λ: Lamé coefficients, σ: stress tensor, κ: thermal conductivity, $\mathbf{u}$: displacement, T: temp.,

Discretization : finite element method (tetrahedral mesh, piecewise linear functions (hp))

Influence of shape variations by Taylor expansion

Truncated polynomial chaos (PC) response surface model

Stochastic variables (Ω, Σ, μ): $\mathbf{p}(\xi) = (p_1(\xi), \dots, p_Q(\xi))$, $\mathbf{p} : \Omega \to \Pi$,
independent, Gaussian, uniform, beta, etc.

PC expansion: a finite second moment of $y_{\mathrm{n}}, [f_0, \dots, f_{\mathrm{end}}]$:

$$y_n(\mathrm{x}, f; \mathbf{p}) \doteq \sum_{i=0}^{P} \alpha_i(\mathrm{x}, f)\Phi_i(\mathbf{p}), \quad n = 1, \dots, N \tag{3}$$

Shape derivative approximation (assuming a joint PDF ρ exists):

$$\mathbb{E}\left[\frac{\partial y_n}{\partial p_q}\right] \doteq \sum_i \left(\alpha_i \int \frac{\partial \Phi_i(\mathrm{p})}{\partial p_q} \rho d\mathbf{p}\right), \quad n = 1, \dots, N \tag{4}$$

First-order Taylor expansion:

$$y_n(\delta\overline{\mathbf{p}} + \overline{\mathbf{p}}) \doteq y_n(\overline{\mathrm{p}}) + \sum_q \frac{\partial y_n}{\partial \overline{p_q}} \cdot \delta\overline{p_q} + \mathcal{O}(|\delta\overline{\mathbf{p}}|^2), \tag{5}$$

with worst-case scenario: $\delta\overline{\mathbf{p}} \doteq \max_{\mathrm{x} \in D_R} |\mathbf{u}(\mathrm{x})|$

Variance-based sensitivity analysis

Main Sobol indices : $0 \leq S_j \leq 1$ with lower and upper bounds

$$S_j = \frac{V_j}{\mathrm{Var}(f)} \quad \text{with} \quad V_j := \sum_{i \in I_j} |v_i|^2, \quad j = 1, \ldots, Q, \tag{6}$$

I_j : sets $I_j := \{j \in \mathbb{N} : \phi_j(\mathrm{p}) \text{ is not constant in } p_j\}$, $\mathrm{Var}(f)$: the total variance

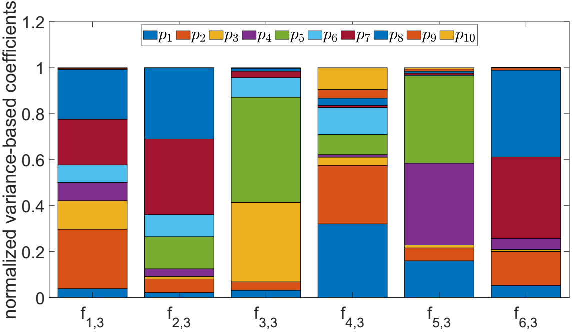

Universität Rostock Traditio et Innovatio

UQ-based worst-case algorithm

Flow of algorithm in the pseudo-code

Algorithm 1 UQ-based worst-case deformation analysis

Initialization :
$\Pi = (p_1, \dots, p_Q)$, $\boldsymbol{\rho}(\mathbf{p})$, $PCtype$, $PCorder$, $\mathbf{w}, \mathbf{p}^{(k)}$,
▷ Eq. (3), PCE param. & gener. weights & poin
for $k = 1 \dots, K$ **do** ▷ Quadrature points loo
  solve MVP($\mathbf{p}^{(k)}$), Eq. (2a) ▷ for eigenpairs **E** &
  solve EVP($\mathbf{p}^{(k)}$), Eq. (2b) ▷ with Eq. (2d) for **u** &
  solve HVP($\mathbf{p}^{(k)}$), Eq. (2c) ▷ for T in deformed
for $i = \{1, \dots, N\}$ **do** ▷ discrete projection loo
  $\alpha_i \leftarrow \langle y_n(\mathbf{p}), \Phi_i(\mathbf{p})\rangle$ ▷ scalar produ
for $q = \{1, \dots, Q\}$ **do** ▷ worst-case shape deformatio
  $\tilde{y}_n \leftarrow \tilde{y}_n + \frac{\partial y_n}{\partial p_q} \cdot \max[|\mathbf{u}_q|]$ ▷ upper boun
Post-processing :
for $i = \{1, \dots, N\}$ **do** ▷ discrete projection loop for $\tilde{y}$
  $\tilde{\alpha}_i \leftarrow \langle \tilde{y}_n(\mathbf{p}), \Phi_i(\mathbf{p})\rangle$ ▷ scalar product for updated $\tilde{y}$
  eval. $\mathbb{E}\left[\tilde{y}_n(\mathbf{p})\right]$, Var $\left[\tilde{y}_n(\mathbf{p})\right]$ ▷ statistical momen
for $q = 1 \dots, Q$ **do**
  eval. $\mathbb{E}\left[\frac{\partial \tilde{y}_n}{\partial p_q}\right]$, S_q ▷ local & global sensitivit

Algorithm for UQ

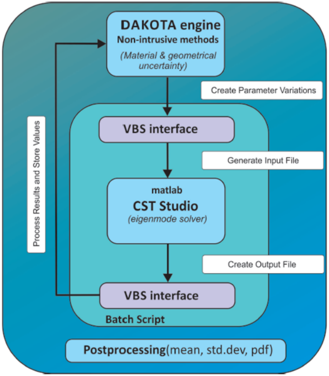

Timeline of ATTAVANTI subproject

Problems & motivation

Stochastic modeling of coupled problem
- Parametrized QPR model
- Unidirectional Stochastic Coupled Problem

UQ-based worst-case analysis for multi-physics QPR simulations
- Influence of shape variations by Taylor expansion
- UQ-based worst-case method

Preliminary results & Conclusions
- Proof-of-concept example
- Results for PDFs of merit-function due to QPR deformation

Parameters of stochastic simulation

Variations of geometrical parameters:

$\longrightarrow$ Modeled by Gaussian distribution, $Q = 8$

Random variations of parameters:

$\longrightarrow$ *gap*: $p_1 = \overline{p}_1(1 + \delta_1\xi_1)$, *wloop*: $p_5 = \overline{p}_5(1 + \delta_5\xi_5)$
$\longrightarrow$ *rrods*: $p_2 = \overline{p}_2(1 + \delta_2\xi_2)$, *dloop*: $p_6 = \overline{p}_6(1 + \delta_6\xi_6)$
$\longrightarrow$ *hloop*: $p_3 = \overline{p}_3(1 + \delta_3\xi_3)$, *rcoil*: $p_7 = \overline{p}_7(1 + \delta_{72}\xi_7)$
$\longrightarrow$ *rloop*: $p_4 = \overline{p}_4(1 + \delta_4\xi_4)$, *rsample*: $p_8 = \overline{p}_8(1 + \delta_{e8}\xi_8)$

- Independent normal random variables: $\xi_1, \xi_2, \xi_3, \xi_4, \xi_5; \xi_6, \xi_7, \xi_8$
- Magnitude of perturbations : $\sigma_i := \delta_i \cdot \overline{p}_i = 0.05\,[\mathrm{mm}], \quad i = 1 \ldots, Q$
- HZB-QPR: $\overline{\mathbf{p}} = (0.5, 13.0, 10.0, 5.0, 44.0, 6.0, 22.40, 37.50)[\mathrm{mm}]$

Lorenz force, air pressure & resulting displacement

Assuming: 1bar pressure, $\iota = 10$, and $k = 3$

- $\overline{\mathbf{p}}^{k=\mathbf{3}} = (0.527, 13.06, 9.93, 4.97, 44.065, 5.973, 22.38, 37.56)[\text{mm}]$
- Worst-case scenario: for $\iota = 10$, $\max[|(\mathrm{u}_{ap} + \iota \cdot \mathrm{u}_{rp})/2|] = 0.1054505$ [mm]

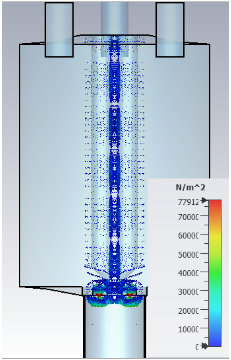

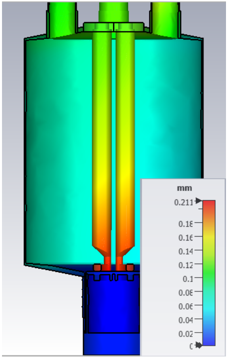

Statistical moments & variance-based decomposition
Means of merit-function:

Name	$\mathbb{E}[f_0(\mathbf{p})]$	$\mathbb{E}[f_1(\mathbf{p})]$	$\mathbb{E}[f_2(\mathbf{p})]$	$\mathbb{E}[f_3(\mathbf{p})]$	$\mathbb{E}[f_4(\mathbf{p})]$	$\mathbb{E}[f_5(\mathbf{p})]$
Unit	[GHz]	[MA^2 / J]	[1/1]	[M1/1]	[1/1]	[mT/(V/m)]
Initial design	1.308	43.006	0.12	0.712	0.932	5.377
Perturbed design	1.320	46.99	0.1293	0.720	0.9124	5.027
Change: $\triangle f_n(\mathbf{p})$	0.008139	-5.429	0.001946	-0.04691	-0.0214	0.11
Change: $\delta f_n(\mathbf{p})(\%)$	0.62 ↑	10.0 ↓	1.53 ↑	6.11 ↓	2.29 ↓	2.56 ↑

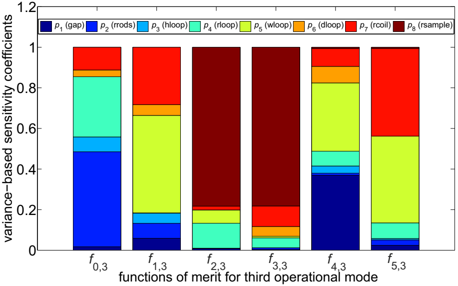

Results for PDFs of merit-function changes:

Estimated change of operating frequency & focusing factor

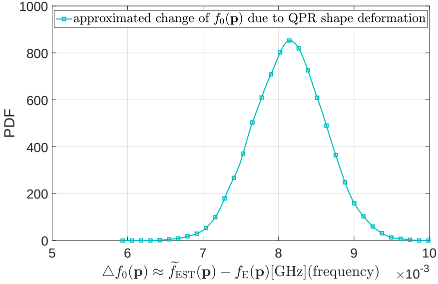

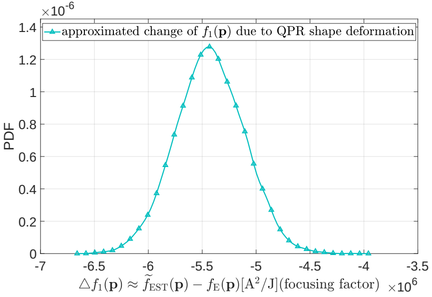

Results for PDFs of merit-function changes:

Estimated change of homogeneity & dimensionless factors

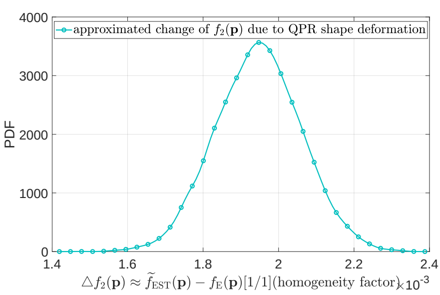

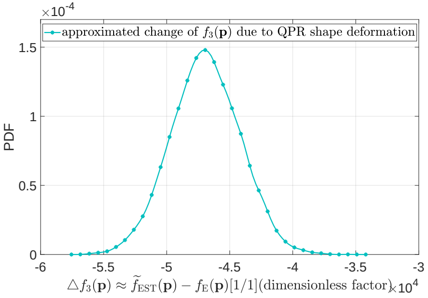

Universität Rostock Traditio et Innovatio

Results for PDFs of merit-function changes:

Estimated change of operating range & risk of field emission

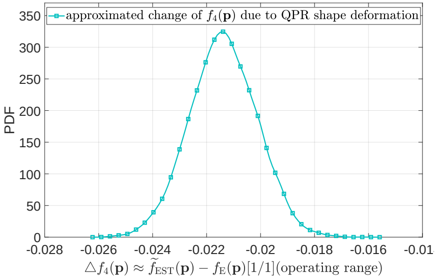

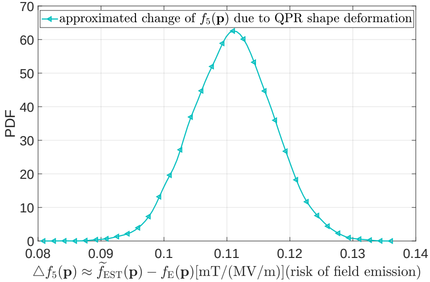

Conclusions and further research

Advantages:

$\longrightarrow$ Reliable simulation for QPRs considering deformation

$\longrightarrow$ Efficient approximation of shape derivatives

$\longrightarrow$ With upper bounds as $\delta\overline{p} := \max_{x \in D_R} |u(x)|$ due to scaled Lorentz force and pressure of 1bar

$\longrightarrow$ Algorithmic complexity: $2 \cdot Q$, Q - no. of paramters

$\longrightarrow$ Good for multi-physics & -objective optimization

Disadvantages:

$\longrightarrow$ Only the worst-case scenario (upper bounds)

$\longrightarrow$ Well approximation of shape derivatives (verified)

$\longrightarrow$ Results of frequency shift can be verified

Further research directions :

$\longrightarrow$ Robust, multi-physics and multi-objective optimization

Thank you for your attention

References

MCCHT03 New instrument to measure the surface resistance of superconducting samples at 400-MHz," *Rev.Sci.Instrum.* 74, 3390–3394, 2003

J12 Investigation of the surface resistance of superconducting materials, Ph.D. thesis, University of Heidelberg, 2012

K17 R. Kleindienst, Radio Frequency Characterization of Superconductors for Particle Accelerators, Ph.D. thesis, University of Siegen, 2017

ABG05 Adjoint methods for electromagnetic shape optimization of the low-loss cavity for the international linear collider, *J. Phys. Conf. Ser.*, 16, 2005

FS00 Steepest descent methods for multicriteria optimization, *Math. Method. Oper. Res.* 51, 2000

LR A multiobjective steepest descent method with applications to optimal well control, *Comput. Geosci.* 20, 2016

PGZWvR Multiobjective design optimization of a quadrupole resonator under uncertainties, *Phys. Rev. Accel. Beams*, 25, 2022

S08 Global sensitivity analysis using polynomial chaos expansion, *Reliab.Eng.Syst.Safe.*, 93, 964–979, 2008